A novel approach to assess the probability of disease eradication from a wild-animal reservoir host

D. P. ANDERSON[1]*, D. S. L. RAMSEY[2], G. NUGENT[1], M. BOSSON[3],
P. LIVINGSTONE[4], P. A. J. MARTIN[5], E. SERGEANT[6], A. M. GORMLEY[1]
AND B. WARBURTON[1]

[1] *Landcare Research, Wildlife Ecology and Management, Lincoln, New Zealand*
[2] *Arthur Rylah Institute, Department of Sustainability and Environment, Heidelberg, Victoria, Australia*
[3] *Animal Health Board, Hamilton, New Zealand*
[4] *Animal Health Board, Wellington, New Zealand*
[5] *Department of Agriculture and Food Western Australia, Bunbury, WA, Australia*
[6] *AusVet Animal Health Services, Orange, NSW, Australia*

SUMMARY

Surveying and declaring disease freedom in wildlife is difficult because information on population size and spatial distribution is often inadequate. We describe and demonstrate a novel spatial model of wildlife disease-surveillance data for predicting the probability of freedom of bovine tuberculosis (caused by *Mycobacterium bovis*) in New Zealand, in which the introduced brushtail possum (*Trichosurus vulpecula*) is the primary wildlife reservoir. Using parameters governing home-range size, probability of capture, probability of infection and spatial relative risks of infection we employed survey data on reservoir hosts and spillover sentinels to make inference on the probability of eradication. Our analysis revealed high sensitivity of model predictions to parameter values, which demonstrated important differences in the information contained in survey data of host-reservoir and spillover-sentinel species. The modelling can increase cost efficiency by reducing the likelihood of prematurely declaring success due to insufficient control, and avoiding unnecessary costs due to excessive control and monitoring.

Key words: Bayes theorem, bovine tuberculosis, eradication, sentinels, surveillance.

INTRODUCTION

Wildlife reservoirs of zoonotic disease continue to present major risks worldwide to human health, domestic animals and endangered wildlife (for review see [1]). Reduction of wildlife disease to low levels is often achievable [2–5], but regional or national disease eradication from wildlife is far more challenging [6–8] and typically requires intensive (and therefore expensive) intervention over large areas for extended periods of time [9, 10]. For such eradication programmes, the key question is deciding when the disease has been eradicated so that wildlife vector control can be stopped. The problem is that the absence of evidence of disease does not necessarily indicate the absence of disease, particularly where little effort has been made to collect evidence. All else being equal, the most cost-effective eradication programme

* Author for correspondence: Dr D. P. Anderson, Landcare Research, Wildlife Ecology and Management, P.O. Box 40, Lincoln 7640, New Zealand.
(Email: andersond@landcareresearch.co.nz)

would be one that stops as soon as the disease has been eradicated. Quantifying the probability of success (i.e. freedom from disease) is crucial in achieving that. Confidence in disease freedom increases with increasing survey effort with negative outcomes across a population. Using surveillance data to predict the probability of disease freedom could reduce the likelihood of prematurely declaring success due to insufficient control and, conversely, could also help avoid incurring unnecessary costs by continuing to fund wildlife vector control long after the disease has been eradicated from an area.

Where surveillance is undertaken to assess the probability that a disease has been eradicated from a host population, the disease will either be confirmed as still present or no disease will be detected. Given negative surveillance results, standard disease survey models for livestock use classical sampling theory to assess the likelihood that a population is free of the disease at a specified prevalence [11–13]. Surveying and declaring disease freedom in wildlife is more difficult. Accurate and precise information on population size (or proportion sampled) and spatial distribution is expensive to obtain and therefore often inadequate. Further, infected populations are often greatly reduced as part of a disease control programme, making it difficult to capture and test hosts even with substantial capture effort, resulting in little information on the population disease status.

In this paper, we describe and demonstrate a spatial model of wildlife disease-surveillance data for predicting the probability of freedom that uses two alternatives to direct sampling of host populations, and hence avoids the estimation of population size and distribution. First, we incorporate an empirically derived probability of host capture that allows a spatially explicit estimate of the probability of disease detection from zero-capture data (i.e. where an effort was made to capture a host but none were captured). Second, we use location data of captured sentinel animals in conjunction with an estimated probability of disease transmission from an infected host to the captured sentinel. We use the term 'host' throughout the paper to mean a true reservoir species capable of independently sustaining the disease of interest [14], and the term 'sentinel' to refer to spillover species that become infected (and so provide a signal of disease presence) but do not play a major role sustaining the disease [15–17].

A virtual grid-cell system is super-imposed over the landscape of interest and the probability of detecting the disease is quantified in each grid cell assuming that the home-range centre of an infected host is in the grid cell. Both sentinels and host-capture devices (e.g. traps) are considered to have 'searched' one or more grid cells for disease as a function of home-range size of sentinels and hosts, respectively, and the probability of disease detection increases with increasing numbers of sentinels surveyed and with increasing effort attempting to capture hosts. The predicted probabilities of detection in each of the grid cells are aggregated up to the landscape using a hierarchical approach that accounts for spatial coverage and spatial relative risks (e.g. due to habitat heterogeneity [18]).

To illustrate this modelling approach, we used surveillance data from the current programme aimed at eradicating bovine tuberculosis (bTB; caused by *Mycobacterium bovis*) from parts of New Zealand [19]. bTB is a globally widespread zoonotic disease of cattle and other livestock, and in New Zealand the introduced brushtail possum (*Trichosurus vulpecula*) has emerged as the primary wildlife reservoir [20–22]. In addition, wild ferrets (*Mustela furo* [23–25]), pigs (*Sus scrofa* [26]) and red deer (*Cervus elaphus scoticus* [27, 28]) have often been found infected but are regarded as spillover hosts at the densities at which they occur in the wild so can be used as sentinels [17]. Specifically, we address three objectives: (1) to describe the probabilistic relationships in the spatial surveillance-data model for quantifying the probability of bTB eradication in possums based on host- and sentinel-surveillance effort; (2) to assess sensitivity of model predictions to model parameters and spatial relative risks; and (3) to quantify the probability of bTB freedom following a localized eradication operation in Blythe Valley, New Zealand using host- and sentinel-surveillance data, and incorporating spatial relative risks.

While we focus on a single system (bTB in possums), the issues encountered here are potentially applicable to many other systems where eradication is a realistic goal [6, 8–10] and surveys do not detect the disease. New Zealand currently spends NZ$82 million annually in an effort to control and eradicate bTB [19]. Although the disease incidence in livestock herds has been reduced by >95% since 1994, with just 0·2% of herds currently infected, about 40% of New Zealand (~10 million ha) is still designated as being vector risk areas in which bTB might still persist in wild possums that could potentially re-infect livestock. As a step toward nationwide biological eradication

of the disease, the current objective of bTB management is to achieve and objectively demonstrate, by 2025, bTB freedom in 2·5 million ha of vector risk areas. Meeting this objective requires a way of quantitatively estimating the probability of freedom for specified areas, a need that prompted the development of the spatial model of wildlife disease-surveillance data.

METHODS

Predicting probability of freedom from bTB in a wild possum population

Possums are a small (2–3 kg) marsupials that were introduced from Australia and are now found in most parts of New Zealand. They are predominantly arboreal folivores and tend to be most abundant in forest (where densities of 5–10/ha are not uncommon) but occur in most other habitats except completely open large areas where there is little or no shrub or tree cover (such as extensive cropland). Infected populations usually have a low prevalence of bTB (1–2% [20]) and are usually surveyed for disease presence using leg-hold trapping.

While our predictive modelling of the probability of disease freedom is novel, it is analogous to the well-established scenario-tree modelling for predicting disease freedom [11–13]. Our modelling approach is organized such that the basic sampling unit is a spatial grid cell that is one of a grid-cell system superimposed on the area of interest (extent). Following a survey in which disease is not detected (S^-; negative surveillance), the probability of bTB freedom for the full extent at time t, $P(\text{free}|S^-)_t$, is calculated as a function of the sensitivity of the surveillance system (SSe_t), or the probability of detecting bTB given an infected possum is present in at least one grid cell. Assuming that false-positive results are not possible (we cannot find bTB if it is not present), Bayes theorem is used to estimate a posterior distribution of $P(\text{free}|S^-)_t$:

$$P(\text{free}|S^-)_t = \frac{P(\text{free})_t}{1 - SSe_t(1 - P(\text{free})_t)}, \qquad (1)$$

where $P(\text{free})_t$ is the prior probability of freedom for the full extent, which can be derived from previous analyses, expert opinion or drawn from a non-informative distribution [e.g. uniform (0,1)]. The $P(\text{free})_t$ and SSe_t are distributions from which we sample to obtain the posterior distribution $P(\text{free}|S^-)_t$. The prior is updated annually, so that the $P(\text{free}|S^-)_t$ becomes the following year's prior [$P(\text{free})_{t+1}$]. If present, the risk of introduction [$P(\text{intro})_t$] from adjacent areas can also be incorporated into the annual updating of the priors:

$$P(\text{free})_t = P(\text{free}|S^-)^*_{t-1} \, (1 - P(\text{intro})_t), \qquad (2)$$

The SSe_t is calculated by combining all cell-level sensitivities (SeU_i; probability of detecting bTB in grid cell i given it is present). The probability of finding an infected grid cell in any order is given by a hypergeometric distribution [29], which is achieved by sampling without replacement each grid cell with its associated SeU_i. To increase computational efficiency, we used a binomial approximation to the hypergeometric distribution to calculate SSe_t [29]:

$$SSe_t = 1 - \left(1 - SeU\text{avg}*\frac{n}{N}\right)^{P^*_u \cdot N}, \qquad (3)$$

where SeUavg is the average grid-cell sensitivity of sampled cells, n is the number of grid cells sampled, N is the total number of grid cells across the full extent, and P^*_u is the grid cell-level prior or design prevalence [12, 13]. The P^*_u is not related to the actual prevalence of disease and is used to determine the amount of surveillance necessary to achieve the eradication goal [13]. The P^*_u is expressed as the minimum proportion of the total number of grid cells expected to be infected if the extent of interest is in fact infected. We use equation (1) to test the hypothesis that that population (of grid cells) is infected at the design prevalence. If we obtain a high $P(\text{free}|S^-)_t$, the likelihood of this hypothesis is low and we can conclude that the population is not infected at or above the design prevalence, but we cannot conclude that it is not infected with a prevalence less than P^*_u. Consequently, to obtain a posterior probability of absolute freedom, the P^*_u must be $1/N$ (i.e. no grid cells contain the home-range centre of an infected possum).

In equation (3), all grid cells are considered to have equal risk of being infected. If the landscape is heterogeneous in terms of habitat suitability for possums or from population control history, then not all grid cells would be expected to have equal risk of infection. Put simply, and in the extreme, if grid cells with a particular habitat do not contain any possums, then bTB cannot be present in those grid cells. Incorporating cell-specific relative risks of infection into the calculation of the SSe_t is achieved with the following equation:

$$SSe_t = 1 - \left(1 - SeU\text{avg} \cdot \frac{n}{N}\right)^{\text{EPIavg} \cdot N}, \qquad (4)$$

where

$$\text{EPIavg} = \frac{P_u^* \sum_{k=1}^{n} \text{AR}_i}{n}, \qquad (5)$$

and AR_i is the adjusted risk for grid cell i. The EPIavg is the effective probability of infection and represents the probability that one of the sampled grid cells is infected. The AR_i is calculated as:

$$\text{AR}_i = N \cdot \text{RR}_i / \sum_{k=1}^{N} \text{RR}_k, \qquad (6)$$

where RR_i is the relative risk for grid cell i. The RR_i are specified relative to the lowest risk grid cell within the spatial extent of interest. If a habitat preference map is used, then high map values suggest relatively high numbers of possums and associated high risk of bTB relative to habitat areas with low preference. The RR_i values can be calculated from a possum habitat map as follows:

$$\text{RR}_i = \frac{\text{habitat}_i}{\min(\text{habitat})}, \qquad (7)$$

where habitat_i is the value that summarizes the habitat preference for grid cell i.

Possum traps and captured sentinels provide information on the probability that bTB is present. We assume that if a possum population is infected, then sympatric spillover hosts such as pigs, ferrets, and deer will also become infected at some level. Sampling of 'sentinel' species therefore provides information on the probability that bTB is in the area. Similarly, if an infected possum was present in an area and the area was surveyed using traps, there is a joint probability that it would be captured and that bTB infection would be detected. Thus, provided no bTB is found, the trapping outcomes also provide information on the probability that bTB is present in possums in the area, regardless of whether or not a possum was actually captured (provided all possums captured within a survey are found to be negative).

Our objective is to use possum traps and sentinels to quantify the probability of detecting bTB in a grid cell given that it is present. We assume that each possum trap j or captured sentinel j 'searches' for bTB in multiple grid cells as a function of home-range size and other parameters (see details below). The SeU_i is calculated as a function of the search effort from one or more traps and sentinels:

$$SeU_i = 1 - \prod_{J=1}^{j} (1 - SeU_{ij}), \qquad (8)$$

where SeU_{ij} is sensitivity of trap/sentinel j detecting bTB in grid cell i. The mechanisms by which possum traps and captured sentinels detect disease in a grid cell are distinct, and therefore we model separately the contribution that these two groups make to grid-cell sensitivities.

The contribution to the SeU_i that is made by a single trap (whether a possum was trapped or not) is simply the product of the probability of capture [$P(\text{capture})_{ij}$] of a possum from cell i in trap j, and the probability that the diagnostic test will detect bTB in an infected animal [$P(\text{test}^+)$]:

$$SeU_{ij} = P(\text{capture})_{ij}\, P(\text{test}^+). \qquad (9)$$

The probability of capture of an infected possum, and therefore the contribution that a trap makes to the sensitivity of a given grid cell will decrease with increasing distance between the trap and the grid cell. We emphasize that equation (9) represents the sensitivity of surveillance using traps, therefore the probability of capture is applied to all traps regardless of whether possums are captured (provided that captured possums are tested and found to be negative).

The probability of trap j capturing an infected possum that has its home-range centre in cell i is calculated as:

$$P(\text{capture})_{ij} = 1 - \left(1 - g_0 \exp\left(\frac{-d_{ij}^2}{2\sigma^2}\right)\right)^{\text{nights}}, \qquad (10)$$

where d_{ij} is the distance between a given trap j and cell i, g_0 is the probability of capturing a possum if the trapping device is placed at the animal's home-range centre [30], σ is the spatial-decay parameter for a home-range kernel [30], and nights represents the number of nights that a trap is set and checked. Consequently, the estimated search effort of a given possum trap for bTB in grid cells is assumed to decay spatially from the trap location with a half-normal kernel up to a maximum distance of twice the radius of a typical possum home range from the trap (4σ).

For spillover sentinels, we assume that individuals are killed and necropsied with an estimated probability of detection of the disease if the animal was infected [$P(\text{test}^+)$]. Unlike traps, we do not use non-capture sentinel survey data in calculating the contribution that captured sentinels make to the SeU_i, because we do not make any assumptions concerning the presence of sentinels, nor do we have any data on the probability of sentinel presence. Thus, because we only use data from animals actually sampled, it is not

Table 1. *Default and range of parameter values used in sensitivity analysis of the wildlife disease-surveillance model. Single parameter values were used, and uncertainty was not incorporated into this analysis*

Parameters	Parameter description	Default value	Sensitivity range
σ	Home-range kernel	90 m	50–130
g_0	Maximum probability of capture	0·13	0·05–0·25
λ_0†	Maximum probability of transmission	0·21	0·05–0·35
$P(\text{test}^+)$	Diagnostic sensitivity	0·95	0·55–0·95
P_u^*	Design prevalence	0·0004	0·0004–0·003
Grid-cell size	Spatial resolution	1 ha	50–125

† Sensitivity analysis of λ_0 was conducted by randomly placing four pigs in the landscape, as λ_0 only applies to spillover sentinel species. The default σ value used for pigs was 910 m, and all other relevant default parameters were as in this table.

necessary to include the probability of capturing sentinels, as we did with possums. We model the probability of detecting bTB in possums in grid cell i using a captured sentinel at location j, therefore we must include the uncertainty associated with the probability of disease transmission from an infected possum in a given grid cell to the sampled sentinel. The probability of a sentinel becoming infected in a given grid cell decreases with increasing distance from the point of capture. The contribution that a captured sentinel j makes to the sensitivity of a given grid cell i is:

$$SeU_{ij} = \left[1 - \left(1 - \lambda_0 \exp\left(\frac{-d_{ij}^2}{2\sigma^2} \right) \right)^{\text{age}} \right] P(\text{test}^+), \quad (11)$$

where λ_0 is the probability that a sentinel becomes infected given that the sentinel's home-range centre is at or very near the home-range centre of an infected possum, and age is the estimated age of the sentinel in years at the time of capture. The exponential term reduces the probability of becoming infected with increasing distance using a half-normal kernel up to a maximum distance of twice the radius of a typical sentinel home range from the capture location (4σ). This search area is selected because we do not have information on the location of the home-range centre. We estimated λ_0 by first calculating the average annual probability that a sentinel would be infected by a single possum occurring within its home range (P_a [31, 32], unpublished data). For each sentinel species and its associated σ, λ_0 was the maximum value (y intercept) of a half-normal distribution with mean P_a.

Parameter sensitivity analysis

We conducted a sensitivity analysis of model parameters to assess how variations in values influence the resulting SSe_t. We evaluated each parameter iteratively across a range of values while holding all other parameters at default values (Table 1). To assess relative parameter sensitivities, the estimated median SSe_t was graphed against the proportional change in parameter value (elasticity [33]). This analysis was done on a simulated square 25-km² landscape with a grid-cell size of 1 ha, and no spatial relative risks were present.

The grid-cell size defines the structure of the model and is not a biological parameter, and the model should not be sensitive to structural parameters. The model and predictions of SSe_t will be insensitive to grid-cell size if P_u^* is adjusted to always be $1/N$. This is appropriate because the objective is to calculate the probability of absolute freedom (i.e. no grid cells contain the home-range centre of an infected possum). The P_u^* was adjusted to be $1/N$ for each grid-cell size in the sensitivity analysis (Table 2).

Last, we conducted a sensitivity analysis of trap placement in landscapes with spatial relative risks of bTB infection (RR). The 25-km² landscape had a baseline RR of 1 and was covered by a varying proportion of a second habitat type (X; Fig. 1). Estimated SSe_t values were graphed across a range of proportions of traps in habitat X (0–100%). In the first test, X was set to cover 50% of the landscape and we compared estimated SSe_t values when RR(X) = 50, 10, 3·33 and 0 (i.e. no RR). The no-RR test was conducted to explore the effect of non-even placement

Table 2. *Details and results of a sensitivity analysis of grid-cell size on a square 25-km² simulated landscape with 50% coverage of a habitat X with a relative risk of 10*

Grid-cell size (length of side)	50 m	75 m	100 m	125 m	
P_u^*	0·0001	0·00023	0·0004	0·00062	
Number of cells	10000	4489	2500	1600	
Number of infected cells	1	1	1	1	
Proportion of traps in habitat X	SSe_t	SSe_t	SSe_t	SSe_t	CV
0	0·249	0·250	0·248	0·252	0·007
0·1	0·261	0·262	0·261	0·264	0·005
0·2	0·277	0·277	0·276	0·279	0·005
0·3	0·283	0·285	0·282	0·284	0·005
0·4	0·287	0·289	0·287	0·288	0·003
0·5	0·286	0·288	0·287	0·286	0·003
0·6	0·289	0·291	0·289	0·288	0·004
0·7	0·284	0·287	0·285	0·283	0·006
0·8	0·280	0·282	0·281	0·279	0·005
0·9	0·282	0·284	0·282	0·280	0·006
1·0	0·379	0·383	0·380	0·381	0·004

Four different grid-cell sizes and associated P_u^* values across a varying range of proportion of traps in habitat X were explored. The SSe_t was calculated for each trial and the coefficient of variation (CV) was calculated across trials with different grid-cell sizes. A lack of effect of grid-cell size is indicated by low CV values for trials across grid-cell sizes (across rows). As expected, SSe_t increases with increasing percentage of landscape covered by traps (down columns).
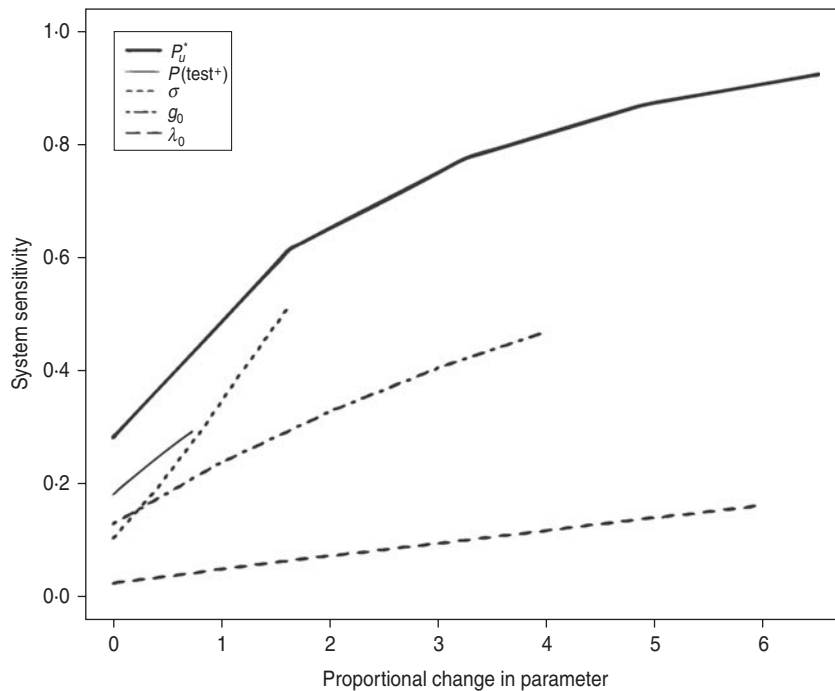

Fig. 1. The estimated median SSe_t was graphed against the proportional change in parameter value (elasticity) to assess the relative sensitivities of parameters. This analysis was done on a simulated square 25-km² landscape with a grid-cell size of 1 ha, and no spatial relative risks were present.

of traps across the landscape. Next we examined the effect of placing a range of proportion of traps in habitat X when RR(X) = 10 and the percentage of cover of habitat X was 20% and 80%. Third, we assessed the effect of placing a varying proportion of 250, 500, 1000 and 1500 traps in habitat X when

Table 3. *Mean and standard deviation of distributions for parameters used in surveillance-data modelling in the Blythe Valley case study*

Species	Mean σ	S.D. σ	Mean g_0	S.D. g_0	Mean $P(\text{test}^+)$	S.D. $P(\text{test}^+)$	Mean λ_0	S.D. λ_0
Possum	90*†	8	0·13*	0·05	0·95	0·10	n.a.	n.a.
Ferret	287*	10	n.a.	n.a.	0·95	0·10	0·081§	0·05
Pig	910*	25	n.a.	n.a.	0·95	0·10	0·21‡	0·10

σ, Home-range size parameter; g_0, probability of capture at home-range centre; $P(\text{test}^+)$, diagnostic sensitivity; λ_0, probability of disease transmission from a possum to a sentinel with home-range overlap; n.a., not applicable.
Source of parameter values: * [40], † [34], ‡ [32], § unpublished data.

RR(X) = 10 and habitat X covered 50% of the landscape.

Case study: Blythe Valley

Blythe Valley is an ~13 000-ha bTB vector control zone in the South Island of New Zealand (173·287°, −42·954°), in which NZ$0·6 million was spent on reducing possum and ferret populations from 2000 to 2009. The area is comprised of pastureland with a mosaic of patches of shrubland and forest, which were the main possum habitat. The surveillance data consisted of 81, 2382, 2642 and 2054 possum traps, and 18, 53, 34 and 37 ferrets captured in the years 2006–2009, respectively. The number of possums killed annually decreased from >3700 in 2000 to 17 in 2009. No bTB has been detected in possums or ferrets since 2004. We applied the spatial bTB surveillance model to possum-trapping and sentinel ferret-necropsy data during the period 2006–2009 to predict the probability of bTB freedom. Although no capture data exist for pigs, we simulated three pig captures per year at random locations in the Blythe Valley for comparative purposes and to illustrate the effect of using multiple data sources on bTB-freedom predictions.

We set grid-cell size to 1 ha and P_u^* to $1/N$ (0·000077). Grid-cell size should be smaller than the expected possum home-range size, and 1 ha was appropriate given that forest-dwelling possums at low density have mean home-range sizes of ~9 ha [34]. To examine the effect of including habitat-based relative risks in the surveillance modelling, we used a predictive spatial model of possum-carrying capacity based on 36 vegetation classes [35]. Relative risk values in our study area varied from 1 to 24.

We accounted for uncertainty in model parameters by repeating the model 500 times, and with each iteration new parameter values were drawn for each possum trap or sentinel from the respective distributions (Table 3). The spatial-decay parameters (σ) were drawn from a normal distribution with a mean and standard deviation for each species (Table 3). The parameters g_0, λ_0, and $P(\text{test}^+)$ were drawn from beta distributions where α and β were derived from a mean and standard deviation (Table 3). The initial prior probability of freedom was drawn in each iteration from a beta distribution derived from a mean = 0·5 and standard deviation of 0·2. Given that the intensive possum control history had probably resulted in a >95% reduction in the possum population over the 2000–2006 period, this is a highly 'pessimistic' or conservative prior as modelling predicts that sustained reduction in possum density of this magnitude is likely to quickly eliminate bTB from possum populations (see [36]).

The posterior $P(\text{free}|S^-)_t$ distribution created by 500 model iterations encompasses parameter uncertainty, which is expressed as credible intervals (CIs). Given uncertainty in model predictions, it is critical to evaluate both the central tendency and the spread of the predictions. We assessed the posterior distributions by evaluating the median, 90% CIs, and the credible interval value (CIV [37]). The CIV examines the posterior distribution by asking what proportion of the posterior probability of freedom is >0·90 (CIV threshold), thus incorporating both the central tendency and the spread in the distribution. Using a CIV threshold of 0·90, we compared results of the Blythe Valley analysis to a target CIV value of 0·95, or the probability that 95% of the posterior $P(\text{free}|S^-)_t$ distribution is >0·90.

RESULTS

The parameter sensitivity analysis demonstrated that variation in home-range size (i.e. σ) has the strongest effect on SSe_t, as indicated by the steepest slope in the
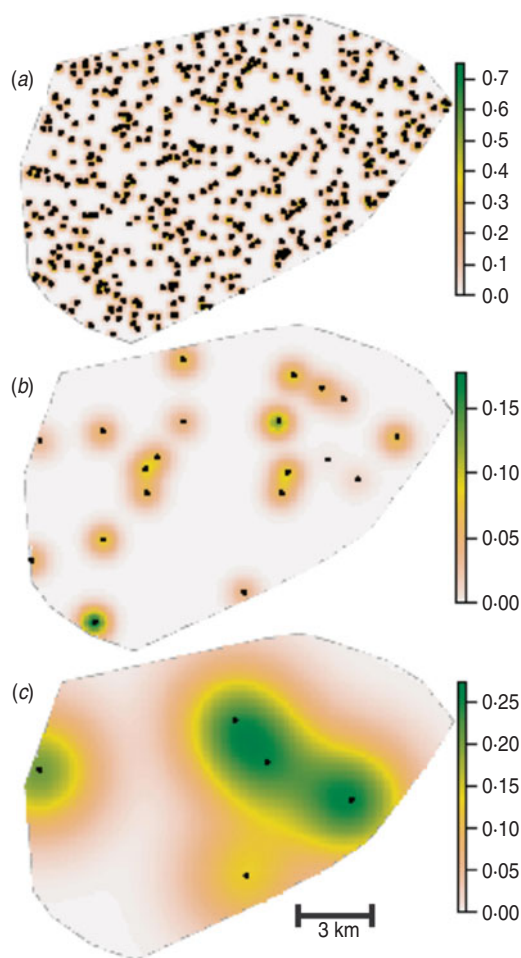
Fig. 2. Maps of grid-cell sensitivities (SeU_i) across the Blythe Valley study area for randomly generated locations for (a) 200 possum traps, (b) 20 ferrets, and (c) five pigs. The black dots are trap locations and the colour scale from green to off-white represents decreasing SeU_i values.

graph of SSe_t against proportion change in parameter values (Fig. 1). Design prevalence (P_u^*) was the next most influential, followed by test sensitivity [$P(\text{test}^+)$], probability of capture at home-range centre (g_0), and probability of infection at home-range centre (λ_0). We illustrated the effects of high parameter sensitivity by plotting the SeU_i for randomly located possum traps, ferrets and pigs in the Blythe Valley study area (Fig. 2). The bTB detection capabilities of the different methods (possum traps, sentinel ferrets, pigs) vary because of their associated parameters. Possums have relatively small home ranges compared to pigs and ferrets (σ in Table 3), therefore possum traps have relatively high grid cell-level sensitivity but in a limited area (Fig. 2a), resulting in a patchy search coverage for bTB. Pigs are effective sentinels because they have large home

ranges (Fig. 2c). Ferrets 'search' areas of intermediate size, but the associated grid cell-level sensitivity is lower than for pigs because of the relatively low λ_0 (Table 3, Fig. 2b).

The sensitivity analysis of SSe_t demonstrated that when P_u^* was maintained at $1/N$, the model predictions did not change with varying grid-cell size (Table 2). The coefficient of variation was <0·008 across trials with different grid-cell sizes and proportion of traps in a habitat that covered 50% of the area and had a RR of 10 (habitat X) vs. the baseline risk of 1.

Several important patterns emerged from the sensitivity analysis of trap placement in simulated landscapes with spatial relative risks (Fig. 3). First, there was usually a local maximum in the SSe_t when detection devices (possum traps in this case) were distributed evenly across the landscape and this was most evident when there was no spatial variation in bTB risk (RR = 0; Fig. 3b). Second, there was a pronounced increase in the SSe_t when most or all of the traps were placed in the high-risk habitat (habitat X; Fig. 3b–d). Third, the SSe_t decreased when a very low proportion of traps were located in the high RR area (Fig. 3b–d). Fourth, when the RR values in habitat X were varied, the respective decrease and increase in SSe_t with low and high proportions of traps in habitat X were related to the RR value (Fig. 3b). Fifth, the rate of increase in SSe_t when most or all the traps were placed in habitat X increased with decreasing percent coverage of habitat X (Fig. 3c). Last, the local maximum of SSe_t with even distribution of traps increased with increasing number of traps, or the ability to search the entire landscape (Fig. 3d). The only explored scenario in which the overall maximum of SSe_t occurred at even-trap distribution was when 1500 were deployed (complete coverage). In contrast, there was no local maximum at even-trap distribution when there were only 250 traps (i.e. very low coverage).

The Blythe Valley case study demonstrated how multiple data sources influence the SSe_t and posterior $P(\text{free}|S^-)_t$ (Table 4). When possum-trapping data were analysed alone, the CIV value in 2009 (0·94) fell just short of the target value of 0·95. The addition of ferret capture data increased the SSe_t and $P(\text{free}|S^-)_t$ for all years, and the CIV value exceeded the target in 2009. The SSe_t and $P(\text{free}|S^-)_t$ increased further for all years with the addition of just three pig captures per year, but the addition of spatial relative risks had little impact on the posterior distributions and the CIV.
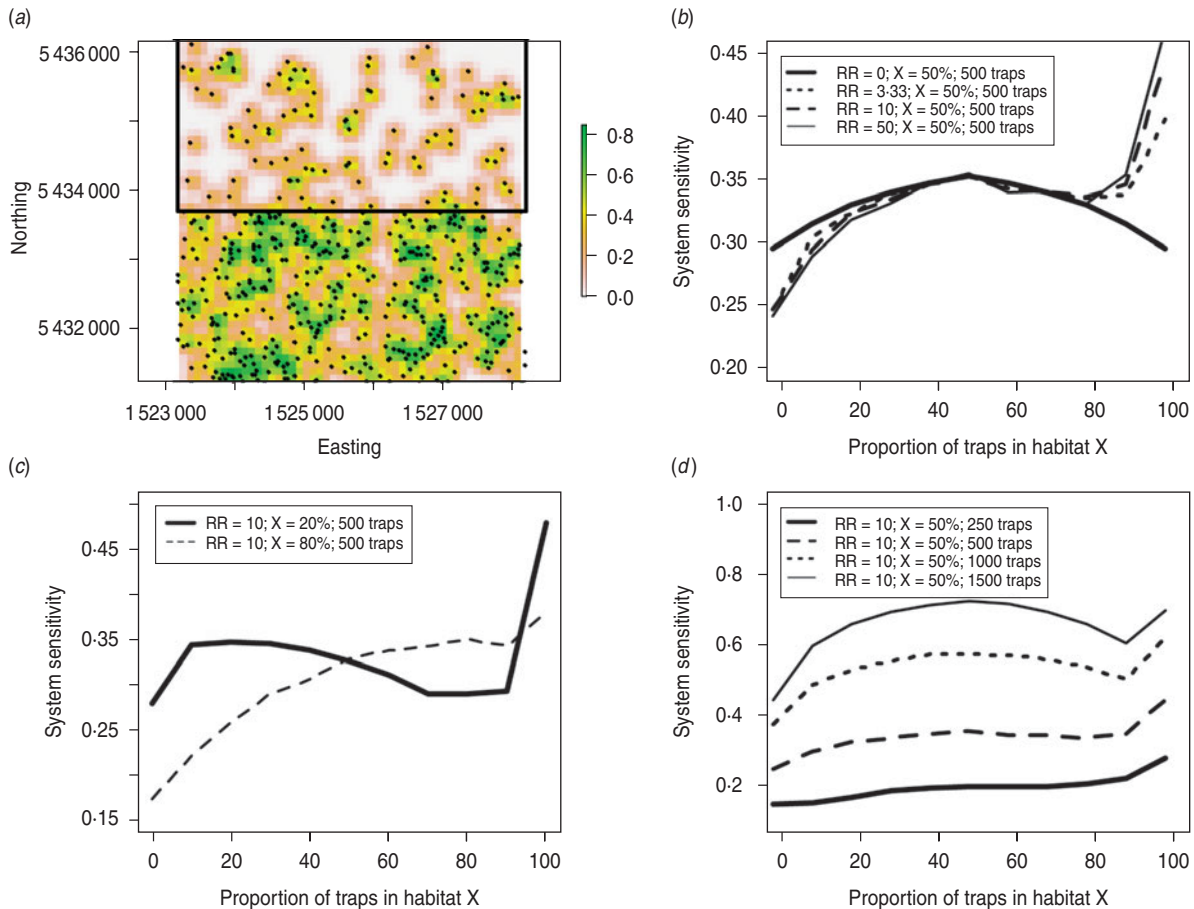
Fig. 3. Design and results of sensitivity analysis of varying trap distribution in simulated landscapes with spatial relative risks (RR). This analysis was performed on a square 25-km² landscape with a grid-cell size of 1 ha, a baseline RR of 1, and a varying RR value in habitat X (*a*). In the example shown here (*a*), 20 % of the possum traps are in habitat X, which makes up 50 % of the landscape. The grid cell-level sensitivities range from >0·8 (green) to 0 (off-white). In this analysis we varied the RR values in habitat X (*b*), proportion of landscape covered by habitat X (*c*), and the number of traps deployed (*d*).

DISCUSSION

We have described and demonstrated a novel spatial model of wildlife disease-surveillance data for predicting the probability of freedom in a wildlife population. By using a spatial grid cell as the basic unit of disease surveillance instead of individual animals, any need to quantify population size and distribution is avoided. Further, data from disparate and unrelated sources, such as sentinel surveillance and host-trapping data (including non-captures), can be combined because sentinels and host capture devices both 'search' the spatial grid cells for the disease. The major advantage of the modelling approach presented here is that while all captured animals are tested for disease, it takes advantage of disease-surveillance effort that does not capture host animals. While possum traps were used here, a variety of animal-capture and disease-detection methods could be used in which

surveillance effort is quantified but wildlife hosts are not always captured.

Our analysis revealed that SSe_t was sensitive to variation in model parameters, and consequently the composition of disease-detection methods and the specified parameter values will have a large influence on model predictions. The SSe_t was most sensitive to σ, which intuitively indicates that SSe_t increases with increasing search area of the device or sentinel. Given the high sensitivity to σ, it is important to have accurate parameter estimates for the area under examination, as home-range sizes vary with population density and habitats [34, 38, 39].

When present for capture, pigs are very efficient sentinels because they have large home ranges [39] and readily acquire the disease if infected possums are present [15]. This was evident in the Blythe Valley analysis in which an addition of only three pigs per year resulted in substantial increases in SSe_t (Table 4).

Table 4. *Results of surveillance-data modelling of Blythe Valley data from 2006 to 2009. Shown are the median, 5th and 95th quantiles of $P(\text{free}|S^-)_t$ and SSe_t, and the credible interval value (CIV) for $P(\text{free}|S^-)_t$ for each year and trial*

Year	$P(\text{free}|S^-)_t$ median	$P(\text{free}|S^-)_t$ 5th quantile	$P(\text{free}|S^-)_t$ 95th quantile	CIV	SSe_t median	SSe_t 5th quantile	SSe_t 95th quantile
Possums only							
2006	0·515	0·342	0·691	0·000	0·026	0·024	0·028
2007	0·733	0·567	0·853	0·000	0·618	0·613	0·622
2008	0·883	0·789	0·942	0·350	0·654	0·649	0·659
2009	0·945	0·898	0·972	0·940	0·594	0·590	0·600
Possums and ferrets							
2006	0·525	0·343	0·666	0·000	0·043	0·039	0·048
2007	0·749	0·586	0·840	0·010	0·635	0·631	0·640
2008	0·894	0·805	0·936	0·430	0·666	0·661	0·670
2009	0·951	0·905	0·971	0·960	0·608	0·603	0·614
Possums, ferrets and pigs							
2006	0·537	0·380	0·689	0·000	0·110	0·078	0·156
2007	0·776	0·643	0·867	0·025	0·668	0·653	0·685
2008	0·916	0·849	0·951	0·695	0·693	0·682	0·708
2009	0·965	0·935	0·981	1·000	0·639	0·625	0·656
Possums, ferrets, pigs and relative risks							
2006	0·521	0·340	0·685	0·000	0·091	0·070	0·118
2007	0·753	0·599	0·858	0·000	0·651	0·637	0·668
2008	0·905	0·826	0·950	0·575	0·697	0·684	0·710
2009	0·961	0·927	0·977	0·995	0·642	0·628	0·659

While possum traps can only capture possums from within a small area (because possums do not range widely), they survey that small area with a high sensitivity. The implication is that where possum traps are used for bTB surveillance, the traps must be closely spaced over a large area to ensure adequate spatial coverage, which requires many traps. While that can be expensive, intensive trapping is also often used to keep the possum population under control, in which case the use of trapping data for disease surveillance could be regarded as 'free' information. Another key advantage of our approach is that possum-trapping surveys have the same influence on SSe_t regardless of how many possums are captured, provided that none of captured possums are found to be infected. Of the three survey methods demonstrated here, the modest number of ferret sentinels available made a much smaller contribution to increasing the SSe_t for detecting the disease than did the possum-trapping surveys in the 2007–2009 period. In 2007, the possum-trapping survey cost NZ$42 750, whilst the ferret survey cost NZ$28 500, suggesting that for this area possum trapping provided more cost-effective bTB surveillance. Pigs are rare or absent in Blythe Valley, but if it were socially acceptable and

posed minimal ecological risk, the release of sentinel pigs (as has been done elsewhere [15]) could be more cost-effective than possum trapping.

The second most influential parameter on SSe_t was, which is not subject to uncertainty. Where absolute eradication is the goal, P_u^* should be set to $1/N$ so that the probability that one or more units are infected given negative surveillance results can be quantified. In contrast, if P_u^* is set to $4/N$, for example, the model calculates the probability that $\geqslant 4$ grid cells are infected, but tells us nothing about the probability of $\leqslant 3$ grid cells being infected given negative surveillance. The P_u^* is inextricably linked to and must be set relative to the grid-cell size, which together determine the expected number of infected grid cells that the surveillance system is attempting to detect [exponential terms in equations (3) and (4)].

Predictions of SSe_t were also sensitive to $P(\text{test}^+)$, g_0 and λ_0, which are subject to uncertainty, and model predictions can be made more accurate by improving our estimates of these parameters. Technological advances that enhance diagnostic test sensitivity [$P(\text{test}^+)$] and rates of possum interaction with traps (g_0) will increase SSe_t predictions for a given survey effort, making it easier to declare disease freedom.

Results of the sensitivity analysis of trap placement in simulated landscapes with spatial relative risks reflect a trade-off between maximizing coverage of the landscape and focusing search effort in high-risk habitats. Intuitively and quantitatively a high proportion of the landscape must be sampled to obtain a sufficiently high SSe_t. In our analysis we explored very simple dichotomous landscapes that had low and high relative risks, consequently we cannot comment on how the distribution of search effort would influence predictions in more complex landscapes. Regardless, including relative risks in the modelling should improve the accuracy in the posterior $P(\text{free}|S^-)_t$. When relative risks are incorporated, the predicted SSe_t can increase if most detection effort is in high-risk areas, or decrease if effort is disproportionately in low-risk areas (Fig. 3b). In our analysis of Blythe Valley, the inclusion of relative risks had little impact on the model predictions, probably due to the detection effort being well distributed and low percentage coverage of risky habitat (Fig. 3b, c).

Confidence in model predictions is contingent on the accuracy of model parameters. The modelling approach deals with this weakness by incorporating uncertainty in parameters and propagating it through to the predicted posterior probabilities of disease freedom. Even in the presence of high uncertainty in model parameters, if search effort is sufficient, a high predicted probability of freedom should be obtained. We emphasize the importance of interpreting the central tendency and the spread or uncertainty in the posteriors by using the CIV [37]. While the CIV requires an arbitrary threshold, it is a comprehensive measure of the magnitude of the posterior probability of freedom and our confidence in predictions.

We expect that the accuracy of the possum-bTB surveillance-data model presented here will increase over time, as a result of research currently being conducted. New empirical data will help to refine model parameters, and model validity will increase with testing model predictions against numerous eradication efforts. Specifically, empirical studies are underway to improve our understanding of possum and sentinel home-range size under a variety of conditions, the probability of capturing hosts (possums) with a variety of devices, and the probability of sentinels becoming infected given the presence of infected hosts in their home range. Given the demonstrated importance of spatial relative risks of disease, improving our ability to quantify spatial relative risks will also improve model accuracy.

Wildlife disease eradication is difficult but can be possible if sufficiently intensive disease control measures, such as host culling, can be applied at broad scales for long enough to eliminate the disease [6–10]. The spatial model of wildlife disease-surveillance data presented here provides a new way of evaluating the probability that eradication has actually been achieved in a specified area. This provides a way of objectively deciding when it is safe to cease disease control measures in a local area, so that resources can be re-allocated to areas where the disease is potentially still present. The model can also be used to determine the optimal spatial arrangement of surveys and forecast the effort necessary to declare success. Cost estimates to justify budgets or to assess feasibility within the constraints of limited budgets can be obtained by using the model to evaluate and plan eradication programmes. The practicality of broad-scale eradication can be tested by aiming for and quantitatively demonstrating disease freedom in limited-area proof-of-concept zones, such as is being attempted in New Zealand [19]. If eradication can be achieved in specified areas, projections of required efforts, time and costs for large areas can be estimated. While the case-study analysis presented here was applied at the level of a landscape-scale operational area, the probability of freedom could also easily be assessed for multiple vector-risk areas, whole regions, or even an entire country; although this would require additional hierarchical levels in the model to account for disease clustering at broad scales [11–13].

ACKNOWLEDGEMENTS

DECLARATION OF INTEREST

None.

REFERENCES

1. **Gortázar C, et al.** Diseases shared between wildlife and livestock: a European perspective. *European Journal of Wildlife Research* 2007; **53**: 241–256.

2. **Artois M.** Wildlife infectious disease control in Europe. *Journal of Mountain Ecology* 2003; **7**: 89–97.

3. **Gortazar C, et al.** Disease risks and overabundance of game species. *European Journal of Wildlife Research* 2006; **52**: 81–87.

4. **Karesh WB, et al.** Wildlife trade and global disease emergence. *Emerging Infectious Diseases* 2005; **11**: 1000–1002.

5. **Wobeser G.** Disease management strategies for wildlife. *Revue Scientifique et Technique de l'Office International des Epizooties* 2002; **21**: 159–178.

6. **Radunz B.** Surveillance and risk management during the latter stages of eradication: experiences from Australia. *Veterinary Microbiology* 2006; **112**: 283–290.

7. **Corner LAL, et al.** The re-emergence of *Mycobacterium bovis* infection in brushtail possums (*Trichosurus vulpecula*) after localised possum eradication. *New Zealand Veterinary Journal* 2003; **51**: 73–80.

8. **Tweddle NE, Livingstone P.** Bovine tuberculosis control and eradication porgrams in Australia and New Zealand. *Veterinary Microbiology* 1994; **40**: 23–29.

9. **Caley P, et al.** Effects of sustained control of brushtail possums on levels of Mycobacterium bovis infection in cattle and brushtail possum populations from Hohotaka, New Zealand. *New Zealand Veterinary Journal* 1999; **47**: 133–142.

10. **Coleman JD, Coleman MC, Warburton B.** Trends in the incidence of tuberculosis in possums and livestock, associated with differing control intensities applied to possum populations. *New Zealand Veterinary Journal* 2006; **54**: 52–60.

11. **Martin PAJ.** Current value of historical and ongoing surveillance for disease freedom: Surveillance for bovine Johne's disease in Western Australia. *Preventive Veterinary Medicine* 2008; **84**: 291–309.

12. **More SJ, et al.** Defining output-based standards to achieve and maintain tuberculosis freedom in farmed deer, with reference to member states of the European Union. *Preventive Veterinary Medicine* 2009; **90**: 254–267.

13. **Martin PAJ, Cameron AR, Greiner M.** Demonstrating freedom from disease using multiple complex data sources. 1: A new methodology based on scenario trees. *Preventive Veterinary Medicine* 2007; **79**: 71–97.

14. **Thrusfeld M.** *Veterinary Epidemiology*, 2nd edn. Oxford: Blackwell Science, 1995, pp. 483.

15. **Nugent G, Whitford J, Young N.** Use of released pigs as sentinels for Mycobacterium bovis. *Journal of Wildlife Diseases* 2002; **38**: 665–677.

16. **Nugent G, Yockney IJ, Whitford EJ.** Intraspecific transmission of *Mycobacterium bovis* among penned feral pigs in New Zealand. *Journal of Wildlife Diseases* 2011; **47**: 364–372.

17. **Nugent G.** Maintenance, spillover and spillback transmission of bovine tuberculosis in multi-host wildlife complexes: A New Zealand case study. *Veterinary Microbiology* 2011; **151**: 34–42.

18. **Caley P, Coleman JD, Hickling GJ.** Habitat-related prevalence of macroscopic Mycobacterium bovis infection in brushtail possums (*Trichosurus vulpecula*), Hohonu Range, Westland, New Zealand. *New Zealand Veterinary Journal* 2001; **49**: 82–87.

19. **Animal Health Board.** National bovine tuberculosis pest management strategy (http://ahb.org.nz/LinkClick.aspx?fileticket = EtXpielnfcg%3d&tabid = 97&mid = 928). Animal Health Board, Wellington, New Zealand, 2009.

20. **Coleman JD, Caley P.** Possums as a reservoir of bovine Tb. In: Montague TL, ed. *The Brushtail Possum: Biology, Impact and Management of an Introduced Marsupial*. Lincoln: Manaaki Whenua, 2000, pp. 92–104.

21. **Jackson R, et al.** Naturally occurring tuberculosis caused by *Mycobacterium bovis* in brushtail possums (*Trichosurus vulpecula*). III. Routes of infection and excretion. *New Zealand Veterinary Journal* 1995; **43**: 322–327.

22. **Morris RS, Pfeiffer DU, Jackson R.** The epidemiology of *Mycobacterium bovis* infections. *Veterinary Microbiology* 1994; **40**: 153–177.

23. **Caley P.** Broad-scale possum and ferret correlates of macroscopic *Mycobacterium bovis* infection in feral ferret populations. *New Zealand Veterinary Journal* 1998; **46**: 157–162.

24. **Lugton IW, et al.** Epidemiology of *Mycobacterium bovis* infection in feral ferrets (Mustela furo) in New Zealand. 2. Routes of infection and excretion. *New Zealand Veterinary Journal* 1997; **45**: 151–157.

25. **Ragg JR, Waldrup KA, Moller H.** The distribution of gross lesions of tuberculosis caused by Mycobacterium bovis in feral ferrets (*Mustela furo*) from Otago, New Zealand. *New Zealand Veterinary Journal* 1995; **43**: 338–341.

26. **de Lisle GW.** Mycobacterial infections in pigs. *Surveillance* 1994; **21**: 23–25.

27. **Lugton IW, et al.** Natural infection of red deer with bovine tuberculosis. *New Zealand Veterinary Journal* 1997; **45**: 19–26.

28. **Lugton IW, et al.** Epidemiology and pathogenesis of Mycobacterium bovis infection of red deer (Cervus elaphus) in New Zealand. *New Zealand Veterinary Journal* 1998; **46**: 147–56.

29. **Cameron AR, Baldock FC.** A new probability formula for surveys to substantiate freedom from disease. *Preventive Veterinary Medicine* 1998; **34**: 1–17.

30. **Efford M.** Density estimation in live-trapping studies. *Oikos* 2004; **106**: 598–610.

31. **Caley P, Ramsey D.** Estimating disease transmission in wildlife, with emphasis on leptospirosis and bovine tuberculosis in possums, and effects of fertility control. *Journal of Applied Ecology* 2001; **38**: 1362–1370.

32. **Nugent G.** The role of wild deer in the epidemiology and management of bovine tuberculosis in New Zealand (Ph.D. thesis). Department of Ecology, Lincoln University, Lincoln, New Zealand, 2005, pp. 171.

33. **Dekroon H, et al.** Elasticity – the relative contribution of demographic parameters to population-growth rate. *Ecology* 1986; **67**: 1427–1431.

34. **Pech R, et al.** The effect of poisoned and notional vaccinated buffers on possum (*Trichosurus vulpecula*) movements: minimising the risk of bovine tuberculosis spread from forest to farmland. *Wildlife Research* 2010; **37**: 283–292.

35. **Efford M.** Possum density, population structure, and dynamics. In: Montague TL, ed. *The Brushtail Possum: Biology, Impact and Management of an Introduced Marsupial*. Lincoln: Manaaki Whenua Press, 2000.

36. **Ramsey DSL, Efford MG.** Management of bovine tuberculosis in brushtail possums in New Zealand: predictions from a spatially explicit, individual-based model. *Journal of Applied Ecology* 2010; **47**: 91191–91199.

37. **McBride GB, Johnstone P.** Calculating the probability of absence using the credible interval value. *New Zealand Journal of Ecology* 2011; **35**: 189–190.

38. **Baber DW, Coblentz BE.** Density, home range, habitat use, and reproduction in feral pigs on Santa Catalina Island. *Journal of Mammalogy* 1986; **67**: 512–525.

39. **Saunders G, McLeod S.** Predicting home range size from the body mass or population densities of feral pigs, *Sus scrofa* (Artiodactyla: Suidae). *Australian Journal of Ecology* 1999; **24**: 538–543.

40. **Ramsey D, et al.** The evaluation of indices of animal abundance using spatial simulation of animal trapping. *Wildlife Research* 2005; **32**: 229–237.